HHS Public Access

Author manuscript

Cell Signal. Author manuscript; available in PMC 2017 June 01.

Published in final edited form as:

Cell Signal. 2016 June ; 28(6): 541–551. doi:10.1016/j.cellsig.2016.02.015.

Dual role of vinculin in barrier-disruptive and barrier-enhancing endothelial cell responses

Anna A. Birukova, **Alok S. Shah**, **Yufeng Tian**, **Nurgul Moldobaeva**, and **Konstantin G. Birukov**

Lung Injury Center, Section of Pulmonary and Critical Medicine, Department of Medicine, University of Chicago, Chicago, Illinois 60637, USA

Abstract

Endothelial cell (EC) barrier disruption induced by edemagenic agonists such as thrombin is a result of increased actomyosin contraction and enforcement of focal adhesions (FA) anchoring contracting stress fibers, which leads to cell retraction and force-induced disruption of cell junctions. In turn, EC barrier enhancement by oxidized phospholipids (OxPAPC) and other agonists is a result of increased tethering forces due to enforcement of the peripheral actin rim and enhancement of cell-cell adherens junction (AJ) complexes promoting EC barrier integrity. This study tested particpation of the mechanosensitive adaptor, vinculin, which couples FA and AJ to actin cytoskeleton, in control of the EC permeability response to barrier disruptive (thrombin) and barrier enhancing (OxPAPC) stimulation. OxPAPC and thrombin induced different patterns of FA remodeling. Knockdown of vinculin attenuated both, OxPAPC-induced decrease and thrombin-induced increase in EC permeability. Thrombin stimulated the vinculin association with FA protein talin and suppressed the interaction with AJ protein, VE-cadherin. In contrast, OxPAPC stimulated the vinculin association with VE-cadherin. Thrombin and OxPAPC induced different levels of myosin light chain (MLC) phosphorylation and caused different patterns of intracellular phospho-MLC distribution. Thrombin-induced talin-vinculin and OxPAPC-induced VE-cadherin-vinculin association were abolished by myosin inhibitor blebbistatin. Expression of the vinculin mutant unable to interact with actin attenuated EC permeability changes and MLC phosphorylation caused by both, thrombin and OxPAPC. These data suggest that the specific vinculin interaction with FA or AJ in different contexts of agonist stimulation is defined by development of regional actyomyosin-based tension and participates in both, the barrier-disruptive an barrier-enhancing endothelial responses.

Keywords

Rho; actin; focal adhesions; vascular permeability; oxidized phospholipids; thrombin; endothelium

Corresponding address: Konstantin Birukov, MD, PhD, Lung Injury Center, Section of Pulmonary and Critical Medicine, Department of Medicine, University of Chicago, 5841 S. Maryland Ave, Office N-611, Chicago, IL 60637, Phone: 773-834-2636, Fax: 773-834-2683, kbirukov@medicine.bsd.uchicago.edu.

1. INTRODUCTION

The vascular endothelium forms a selective permeable barrier between the blood and the interstitial space of all organs and participates in the regulation of macromolecule transport and blood cell trafficking through the vessel wall. Barrier maintenance is determined by the equilibrium of competing contractile and tethering forces generated by the cytoskeletal motor proteins such as actin and myosin and the adhesive molecules located at cell-cell and cell-matrix contacts.

Robust activation of actomyosin contraction by vasoactive agonists and excessive mechanical forces affect endothelial cell (EC) monolayer integrity and increase endothelial permeability. The EC barrier disruptive response resulting from activation of actomyosin contractile activity is accompanied by massive actin stress fiber formation and anchoring of actomyosin contractile machinery to enlarged cell-substrate contact points, the focal adhesions (FA). This process is mediated by the RhoA GTPase pathway [1, 2]. Interaction of activated RhoA with Rho-associated kinase (Rho-kinase) causes activation of Rho-kinase enzymatic activity and phosphorylation of its substrate, the myosin-binding subunit of myosin-associated phosphatase type 1 (MYPT1) [3]. Rho-kinase-mediated MYPT1 phosphorylation inhibits MYPT1 phosphatase activity, increases a pool of phosphorylated myosin light chain (MLC) and triggers stress fiber formation, actomyosin contraction, paracellular gap formation and EC permeability. Activation of RhoA is also essential for the remodeling and enhancement of mechanically loaded FA [4, 5].

In contrast to the contractile mechanism of increased EC permeability, the enhancement of the EC barrier by agonists such as sphingosine 1-phosphate, hepatocyte growth factor or products of phosphoadityl choline oxidation (OxPAPC) is mainly driven by Rac1 and Rap1 GTPases, involves activation of cortical actin polymerization, peripheral cytoskeletal remodeling and strengthening of cell-cell junctions [6–13]. Adherens junctions (AJ) play a key role in the maintenance of EC monolayer integrity and the regulation of EC permeability. Moderate increase in MLC phosphorylation reflecting the activation of cortical contractile activity was observed at the peripheral compartment of EC exposed to barrier enhancing stimuli [14].

Vinculin is a globular protein present in both cell-cell and cell-matrix adhesions [15] and consisting of 5 helical head domains (D1–D5) connected to the vinculin tail domain (Vt) by a flexible linker region [16]. Direct interaction of the head domain (D1) with the tail domain renders a closed, auto-inhibited vinculin conformation. The tail domain contains binding sites for F-actin, paxillin, and PIP_2, while the head domain, D1 holds binding sites for a FA protein talin, F-actin crosslinking protein α-actinin, and AJ protein α-catenin, which are essential for selective vinculin targeting to FA or AJ. In the closed conformation, vinculin is unable to bind both filamentous actin at Vt and talin or α-catenin at D1 [17]. Vinculin is important for transmitting mechanical forces and orchestrating mechanical signaling events [18]. Vinculin appears more stably incorporated in mature FAs experiencing mechanical loads from contracting actomyosin fibers anchored to FA [19]. Vinculin association with talin and actin cytoskeleton is important for the force-induced strengthening of FA, recruitment of additional FA proteins such as paxillin and anchoring contractile stress fibers

[18]. On the other hand, vinculin can incorporate into the cadherin molecular complex [20] and enforce cadherin-based cell–cell interactions, presumably by interacting with α-catenin and linking adherens junctions with actin cytoskeleton [21]. Vinculin interaction with AJ protects VE-cadherin junctions from opening during their force-dependent remodeling [22].

How barrier-disruptive and barrier enhancing signals regulate vinculin interactions with FA and AJ and whether increased anchoring of FA and AJ to the actin cytoskeleton mediated by vinculin is essential for EC permeability responses to barrier-disruptive and barrier-protective agonists remains unclear. This study tested the involvement of vinculin in the mediation of EC permeability responses to barrier-disruptive (thrombin) and barrier-enhancing (OxPAPC) agonists. Using cell imaging, biochemical and molecular approaches we investigated agonist-dependent vinculin association with FA and AJ and examined the involvement of local actomyosin contractility in the vinculin-mediated control of EC permeability by barrier disruptive and barrier enhancing agonists.

2. MATERIALS AND METHODS

2.1. Cell culture and reagents

Human pulmonary artery endothelial cells (HPAEC) and cell culture basal medium with growth supplements were obtained from Lonza Inc (Allendale, NJ), cultured according to the manufacturer's protocol, and used at passages 5–7. 1-Palmitoyl-2-arachidonoyl-sn-glycero-3-phosphocholine (PAPC, Avanti Polar Lipids, Alabaster, AL) was oxidized by exposure of dry lipid to air as previously described [23–25]. The extent of oxidation was monitored by positive ion electrospray mass spectrometry (ESI-MS) as described previously [25]. Blebbistatin was obtained from EMD Millipore (Billerica, MA). All reagents for immunofluorescence were purchased from Molecular Probes (Eugene, OR). Antibodies against di-phospho (Thr18/Ser19) and mono-phospho (Ser19) MLC were from Cell Signaling (Beverly, MA); vinculin and β-actin antibodies were from Sigma (St. Louis, MO); Myosin-A was from Covance (Berkley, CA); talin was from EMD Millipore; VE-cadherin antibody was from Cayman (Ann Arbor, MI). Unless specified, biochemical reagents were obtained from Sigma (St. Louis, MO). YFP-vinculin and YFP-vinc880 mutant which lacks C-terminal F-actin binding domain were a generous gift by C. Ballestrem [26]. EC were used for transient transfections according to the protocol described previously [27]. Transfection efficiency of plasmid DNA was in the 30% range.

2.2. siRNA and DNA transfection

To reduce the content of endogenous vinculin, cells were treated with gene-specific siRNA duplexes. Pre-designed standard purity siRNA sets (*Homo sapiens*) were purchased from Ambion (Austin, TX), and transfection of EC with siRNA was performed as previously described [28]. After 48–72 hrs of transfection, cells were used for experiments or harvested for western blot verification of specific protein depletion. Nonspecific, non-targeting siRNA (Dharmacon, Lafayette, CO) was used as a control treatment. The siRNA transfection efficiency according to our protocol exceeded 90% [11].

2.3. Co-immunoprecipitation and Immunoblotting

Co-immunoprecipitation studies and Western Blot analysis were performed using confluent HPAEC monolayers as described elsewhere [6]. Protein extracts were separated by SDS-PAGE, transferred to polyvinylidene difluoride membranes, and the membranes were incubated with antibodies of interest. Equal protein loading was verified by probing of membranes with antibody to β-actin or a specific protein of interest.

2.4. Immunofluorescence

Endothelial monolayers plated on glass cover slips were treated with the agonist of interest, fixed in 3.7% formaldehyde solution in PBS for 10 min at 4° C, washed three times with PBS, permeabilized with 0.1% triton X-100 in PBS-Tween (PBST) for 30 min at room temperature, and blocked with 2% BSA in PBST for 30 min. Incubations with primary antibody of interest were performed in blocking solution (2% BSA in PBST) for 1 hr at room temperature followed by staining with Alexa 488 or Alexa 594-conjugated secondary antibodies. Actin filaments were stained with Texas Red- conjugated phalloidin. After immunostaining, cell imaging was performed using the Nikon imaging system Eclipse TE 300 (Nikon, Tokyo, Japan) equipped with a digital camera (DKC 5000, Sony, Tokyo, Japan); 60× objective lenses were used. Images were processed with Adobe Photoshop 7.0 software (Adobe Systems, San Jose, CA). Quantification of agonist-induced focal adhesion and adherens junction remodeling was performed as described elsewhere [29–31] using MetaVue 4.6 software (Universal Imaging, Downington, PA). The 16-bit images were analyzed using MetaVue 4.6 (Universal Imaging, Downington, PA). The cells to be analyzed were outlined based on VE-cadherin staining and were divided at 70% radius. The integrated fluorescence density in the peripheral area was measured. Similar methods were applied to focal adhesion quantification in fixed cells except that talin immunoactivity was manually counted and results were not normalized. The values were statistically processed using Sigma Plot 7.1 (SPSS Science, Chicago, IL) software. For each experimental condition at least 10 microscopic fields in each independent experiment were analyzed.

2.5. Measurement of transendothelial electrical resistance

EC monolayer barrier properties were evaluated by the highly sensitive biophysical assay with an electrical cell-substrate impedance sensing system (Applied Biophysics, Troy, NY) that allows measurements of transendothelial electrical resistance in real time, which reflects agonist-induced EC permeability changes [32].

2.6. Statistical analysis

Results are expressed as means ± SD. Experimental samples were compared to controls by unpaired Student's t-test. For multiple-group comparisons, a one-way variance analysis (ANOVA) and post hoc multiple comparison tests were used. $P<0.05$ was considered statistically significant.

3. RESULTS

3.1. Contrasting effects of thrombin and OxPAPC on EC permeability and vinculin distribution

Human pulmonary EC were treated with thrombin or OxPAPC. Measurements of permeability across pulmonary EC monolayers revealed a rapid and pronounced increase in EC permeability reflected by a drop in transendothelial electrical resistance (TER) (Figure 1A). In contrast, OxPAPC induced a pronounced TER increase, reflecting EC barrier enhancement. The morphological response of pulmonary EC to thrombin stimulation was characterized by the enlargement of vinculin-positive FA randomly localized in thrombin-stimulated EC (Figure 1B). In contrast, OxPAPC stimulation induced predominant localization of vinculin immunoreactivity at the cell periphery, in the regions of cell-cell contacts. Recent study by Bays et al. [33] demonstrated selective phophorylation of vinculin localized at adherens junctions at Y822 which was further increased when external forces were applied to AJ. Vinculin phosphorylation at Y822 was not induced by force application to focal adhesions. We next tested if this unique AJ tension-dependent phenomenon can be observed in EC stimulated with barrier-disruptive and barrier protective agonists. Basal levels of phospho-Y822 vinculin we detected by western blot analysis of un-stimulated confluent EC monolayers and were not affected by thrombin stimulation (Figure 1C, **left panels**). In contrast, barrier-enhancing agonist OxPAPC increased phospho-Y822 vinculin levels in pulmonary EC (Figure 1C, **right panels**). Immunofluorescence analysis showed exclusive localization of phospho-Y822 vinculin at the cell border, in the AJ areas (Figure 1D).

3.2. Vinculin association with talin and VE-cadherin is differentially regulated by thrombin and OxPAPC

Because vinculin is a bi-functional cell adhesion protein, which may localize to both, FA and AJ complexes [15], we analyzed vinculin association with talin and VE-cadherin in EC stimulated with OxPAPC and thrombin. Thrombin treatment significantly increased the vinculin association with FA partner talin, which was observed at 5 min and 15 min of thrombin stimulation, the time points corresponding to maximal permeability response, but decreased the VE-cadherin presence in the vinculin immunocomplex at these time points (Figure 2A). In contrast, cell stimulation with OxPAPC increased the vinculin association with both, talin and VE-cadherin at the time points of EC barrier enhancing response. These results were further confirmed by analysis of vinculin colocalization with VE-cadherin in thrombin- and OxPAPC-stimulated EC performed using double immunofluorescence staining. Thrombin treatment disrupted the continuous VE-cadherin staining reflecting impaired cell junctions (Figure 2B) but induced strong vinculin-talin colocalization at enlarged focal adhesions (Figure 2C). In contrast, OxPAPC stimulation promoted vinculin-VE-cadherin and vinculin-talin colocalization at the cell periphery suggesting an increased vinculin presence at AJ (Figure 2B, **right panels**). These results are consistent with co-immunoprecipitation data shown above.

3.3. Vinculin mediates cell adhesion remodeling and EC permeability responses to thrombin and OxPAPC

To evaluate the involvement of vinculin in thrombin- and OxPAPC-induced EC permeability responses, we depleted endogenous vinculin in pulmonary EC using an siRNA approach and measured TER changes upon thrombin or OxPAPC stimulation (Figure 3). Treatment with vinculin-specific siRNA caused approximately 80% decrease in vinculin protein expression, as compared to cells treated with non-specific RNA duplexes (inset in Figure 3). Depletion of vinculin significantly attenuated permeability responses to both, thrombin and OxPAPC treatment as compared to agonist-stimulated cells transfected with non-specific RNA.

Morphological analysis of FA in agonist-stimulated EC with depleted vinculin was performed by immunofluorescence staining of cell monolayers with an antibody to another FA-associated protein and vinculin binding partner talin. Vinculin knockdown significantly decreased the size of FA in thrombin-stimulated EC ($0.59\pm0.19\ \mu m^2$ in nsRNA transfected EC versus $0.11\pm0.07\ \mu m^2$ in si-vinculin transfected EC; $p<0.05$) (Figure 4, **middle panels**). Vinculin knockdown also attenuated the formation of nascent talin-positive peripheral FA in OxPAPC-stimulated EC (Figure 4, **right panels and inset**).

The EC barrier enhancing response to OxPAPC is associated with enlargement of VE-cadherin positive continuous adherens junctions in EC monolayers [6, 34]. Vinculin knockdown significantly reduced the enlargement of VE-cadherin positive areas (Figure 5). These effects are associated with reduced barrier-enhancing response to OxPAPC by pulmonary EC with depleted endogenous vinculin depicted in Figure 3.

3.4. Focal adhesion – cytoskeletal interactions and MLC phosphorylation in thrombin- and OxPAPC-stimulated EC monolayers

FA maturation is associated with increased accumulation of vinculin and talin, which also serve as force transducers bearing physical load exerted by actomyosin fibers [18, 19]. The next experiments tested the patterns of actomyosin-FA arrangement in EC stimulated with thrombin and OxPAPC. Thrombin treatment induced formation of pronounced actin stress fibers attached to the enhanced FAs. A previous study by our group showed an approximately two-fold increase in the average FA size caused by thrombin [35]. In contrast, OxPAPC stimulated formation of a more diffuse peripheral actin rim, which attached to the peripherally localized FAs (Figure 6).

Thrombin-induced MLC phosphorylation is mediated by activation of myosin light chain kinase and Rho-dependent inhibition of myosin phosphatase activity leading to robust accumulation of MLC diphosphorylated at Ser^{19}/Thr^{18} [36]. In contrast, OxPAPC barrier enhancement effects are associated with the activation of Rac1 GTPase [34]. Rac1 may promote monophosphorylation of MLC by Rac1 effector kinase PAK1 [37]. MLC monophosphorylation at Ser19 induces less efficient actomyosin contraction. Western blot analysis of agonist-stimulated EC showed increased di- and mono-phospho-MLC levels in thrombin-treated EC and increased mono-phospho-MLC levels in OxPAPC-stimulated EC (Figure 7A). Immunostaining for mono-MLC using selective phosphospecific MLC antibodies showed a robust increase in phospho-MLC levels localized in the center of

thrombin-stimulated EC. In contrast, OxPAPC treatment increased monophospho-MLC immunoreactivity at the cell periphery (Figure 7B).

The role of actomyosin-generated forces in thrombin- and OxPAPC-induced vinculin interactions with FA and AJ targets was further evaluated in experiments with the inhibitor of myosin ATPase activity blebbistatin. Preincubation with blebbistatin attenuated thrombin-induced association of vinculin with talin and prevented dissociation of vinculin-VE-cadherin complex induced by thrombin. In OxPAPC-stimulated cells, treatment with blebbistatin attenuated vinculin association with both, VE-cadherin and talin (Figure 7C).

3.5. Role of vinculin linkage to actin cytoskeleton for actomyosin activation and EC permeability response to thrombin and OxPAPC

The Vinculin C-terminal tail has been identified as critical domain linking vinculin to the actin cytoskeleton [26]. We expressed the vinculin C-terminus deletion mutant (vinc880) in pulmonary EC to evaluate a role of vinculin linkage to actin cytoskeleton in the vinculin-dependent regulation of EC permeability response to thrombin and OxPAPC. These effects were compared to EC with ectopic expression of full length recombinant vinculin. Ectopic expression of VNC-880 significantly attenuated permeability changes caused by both, thrombin and OxPAPC in comparison to EC expressing full-length vinculin (Figure 8A). Insets in Figure 8A depict expression levels of endogenous vinculin and ectopically expressed VNC-880 and VNC-FL proteins detected by western blot. To account for effects of increased expression of full length vinculin, we also compared agonist-induced TER responses by non-transfected EC and cells expressing VNC-FL. Expression of VNC-FL enhanced both, the TER increase in response to OxPAPC and TER decline in response to thrombin stimulation (Figure 8A). These results emphasize the dual role of vinculin in mediation of barrier-disruptive and barrier-enhancing EC responses. Expression of vinc880 also attenuated mono- and di-phosphorylation of MLC induced by thrombin and mono-phosphorylation of MLC caused by OxPAPC (Figure 8B). In consistence with Figure 7A, OxPAPC did not cause di-phopshorylation of MLC at the indicated time point.

4. DISCUSSION

Published studies show differential patterns of actin cytoskeletal arrangement and intracellular force distribution in EC stimulated with barrier-disruptive and barrier-enhancing agonists [38–41]. Increased cytoskeletal stiffness was registered in central areas of cells stimulated with barrier disruptive contractile agonists. These areas showed increased concentration to actomyosin stress fibers. In turn, in cells stimulated with barrier enhancing agonists, an accumulation of actin cytoskeleton and increased elastic modulus, reflecting the stiffness of the contractile apparatus, was detected at the cell periphery [6, 38, 39]. These effects are also associated with the increased assembly of adherens junction complexes [42, 43]. Because vinculin accumulation may occur in the areas of increased mechanical tension at both, focal adhesions and adherens junctions [15, 44, 45], we hypothesized that vinculin interactions with FA and AJ may be agonist-specific.

The main finding of this study is the demonstration of a dual role of vinculin in modulation of both, barrier-enhancing and barrier-disruptive responses by endothelial cells. The

differential role of vinculin in modulating EC permeability caused by barrier-disruptive and barrier-enhancing agonists was dictated by agonist-specific vinculin localization at FA or AJ, which in turn was driven by agonist-specific patterns of actomyosin remodeling and spatial distribution of intracellular forces.

The thrombin-induced EC permeability response is associated with development of significant contractile forces [40] generated by actomyosin stress fibers spanning the central part of the cell and anchored to the enlarged FA [35]. In response to tension exerted by the cytoskeleton, FA in thrombin-stimulated EC undergo reinforcement reflected by vinculin accumulation [26]. Mechanical forces induce conformational changes in FA-associated scaffolding proteins including vinculin, which unmask cryptic binding sites for additional proteins [46]. Altogether, these processes lead to reinforcement of focal adhesive structures, but may also stimulate recruitment of additional proteins regulating local signaling at FA.

Our data show that thrombin triggered vinculin-dependent enforcement of FA and FA linkage with actin cytoskeleton. These vinculin-dependent events were dependent on actomyosin contractile activity (as shown in experiments with blebbistatin) and vinculin interactions with both, focal adhesions and actin cytoskeleton (as shown in experiments with tailless VNC-880 mutant). Force-induced vinculin activation was also essential for the maximal EC contractile response to thrombin, as demonstrated by reduced MLC phosphorylation and permeability response in thrombin-stimulated EC expressing VNC-880 truncated mutant unable to interact with actin cytoskeleton. It remained unclear what drives vinculin differential localization at cell junctions or focal contacts under different circumstances until recent report by Bays et al. [33], which demonstrated selective vinculin phosphorylation at Y822 in cell-cell, but not cell-matrix, adhesions of epithelial cells. This phosphorylation was enhanced by external forces applied to E-cadherin and required for vinculin integration into the cadherin complex. In contrast, Y822 phosphorylation was not required for vinculin functions in focal adhesions. The results of this study show OxPAPC-induced elevation of phospho-Y822 vinculin levels and selective accumulation of phospho-Y822 vinculin at the enlarged cell junctions of OxPAPC-stimulated endothelial cells. These results together with visualization of peripheral phospho-MLC localization in OxPAPC-treated cells support the specific targeting of phospho-Y822 vinculin to AJ and its potential role in tension-dependent enforcement of AJ as a mechanism of pulmonary endothelial barrier enhancement.

In contrast to thrombin, OxPAPC did not produce generalized cell contraction, but instead stimulated formation of the peripheral actin rim and peripheral accumulation of FA and AJ complexes via Rac1 and Cdc42 GTPase dependent mechanisms [6, 34]. Stimulation with OxPAPC increased vinculin association with both, FA member talin and VE-cadherin at cell border. Our previous reports showed functional association of FA and AJ complexes in OxPAPC-stimulated EC via direct interaction of FA adaptor protein paxillin with AJ-associated β-catenin [6, 47]. These data suggest that, in addition to previously reported vinculin interaction with E- or VE-cadherin based adherens junctions [22, 48], barrier-enhancing agonists promote functional interactions between AJ and FA [6, 49], thus explaining the presence of talin in the vicinity of AJ. Vinculin association with VE-cadherin in OxPAPC-stimulated EC linked AJ to pre-contracted cortical actin cytoskeleton, as

reflected by the increased phospho-MLC levels and the peripheral localization of monophosphorylated MLC in OxPAPC-stimulated endothelial cells. Indeed, direct analysis of cytoskeletal mechanical properties of OxPAPC-stimulated EC using atomic force microscopy approach demonstrated specific mechanical strengthening of the subcortical cytoskeletal compartment [39]. Such a pattern of elevated cortical contractility was also typical for other barrier enhancing agonists such as hepatocyte growth factor, sphingosine 1-phosphate and prostacyclin [38, 39], but it is important to note that the levels of local cytoskeletal contraction were much lower in comparison to effects of barrier-disruptive agonists. Increased levels of mono- but not di-phosphorylated MLC in cortical regions of OxPAPC-stimulated EC may be attributed to the activation of the Rac1 effector, serine/threonine protein kinase PAK1, shown to inhibit the activity of myosin light chain kinase, but phosphorylate MLC directly [37, 50]. We also cannot exclude and additional role of basal Rho activity in promoting the assembly of peripheral actomyosin in OxPAPC-stimulated cells.

Mechanical loading of VE-cadherin at the surface of endothelial cells using VE-cadherin-coated magnetic beads pulled by magnetic field triggered local vinculin recruitment and actin cytoskeletal remodeling [45, 51]. The current study shows that development of cytoskeletal forces at the periphery of OxPAPC-stimulated EC caused by MLC monophosphorylation leads to strengthening of AJ circumventing the cells, which altogether enhance tethering forces between neighbor cells and, as a result, elevate EC monolayer barrier properties. In turn, inhibition of actomyosin motor activity attenuated effects of both, thrombin and OxPAPC on EC permeability and decreased vinculin association with FA and AJ. Our findings are also supported by a reported myosin II role in contractile enhancement of adherens junctions [52]. Overall, the contractile forces developed by peripheral cytoskeleton connected to vinculin-enforced VE-cadherin adherens junctions in EC stimulated with barrier-enhancing agonists appear to match the mechanical strength of cell-cell junctions, which is a critical prerequisite to agonist-induced enhancement of EC barrier. These forces are of significantly lower magnitude in comparison to forces developed by actomyosin stress fibers anchored by enlarged focal adhesions in EC exposed to barrier disruptive contractile agonists such as thrombin, which is also illustrated by the different levels of mono- and diphospho-MLC in these conditions.

It however, remained unclear what drives vinculin differential localization at cell junctions or focal contacts under different circumstances until recent report by Bays et al. [33], which demonstrated selective vinculin phosphorylation at Y822 in cell-cell, but not cell-matrix, adhesions of epithelial cells. This phosphorylation was enhanced by external forces applied to E-cadherin and required for vinculin integration into the cadherin complex. In contrast, Y822 phosphorylation was not required for vinculin functions in focal adhesions. The results of this study show OxPAPC-induced elevation of phospho-Y822 vinculin levels and selective accumulation of phospho-Y822 vinculin at the enlarged cell junctions of OxPAPC-stimulated endothelial cells. These results together with visualization of peripheral phospho-MLC localization in OxPAPC-treated cells support the specific targeting of phospho-Y822 vinculin to AJ and its potential role in tension-dependent enforcement of AJ as a mechanism of pulmonary endothelial barrier enhancement.

In summary, our results show that vinculin association with FA or AJ is agonist-specific, depends on the local development of actomysoin tension marked by increased MLC phosphorylation and is required for the EC permeability response to both, barrier-disruptive and barrier-protective agonists. These results suggest FA as major force-bearing structures in EC stimulated with contractile agonists, although focal points of VE-cadherin positive cell-cell contacts have been also described [22], and may play a role in reannealing of adhrerens junctions during recovery of EC barrier. Vinculin in those conditions reinforces FA, which escalate activation of actomyosin contractile machinery leading to the disruption of intercellular AJ and increased EC permeability. Vinculin is also involved in the cytoskeletal tension - Rho positive feedback mechanism. On the other side, phosphorylation-dependent vinculin targeting and vinculin-assisted force generation at AJ appears to be critical for tightening the AJ structure and enhancement of the EC barrier in cells treated with barrier-protective agonists. These changes reflect establishment of the tension-mounted AJ complex linked to the actin cytoskeleton, which is essential for the sustained enhancement of the EC barrier. These results also suggest a central role for vinculin in the model of endothelial barrier regulation via dynamic balance between centripetal forces imposed by actomyosin-based contraction of stress fibers attached to focal adhesions and tethering forces applied by peripheral cytoskeletal elements and cell-cell adhesive complexes. In both scenarios, vinculin association with FA and AJ protein partners requires certain levels of cytoskeletal tension and can be abolished by myosin motor inhibitors.

Acknowledgments

The authors wish to thank Christopher Ballestrem (University of Manchester) for sharing vinculin constructs. This work was supported by Public Health Service grants HL76259 and HL107920 from the National Heart, Lung, and Blood Institute.

Non-standard Abbreviations

AJ	adherens junctions
EC	endothelial cells
FA	focal adhesions
GEF	guanine nucleotide exchange factor
HPAEC	human pulmonary artery endothelial cells
MLC	myosin light chain
MYPT1	myosin light chain phosphatase
OxPAPC	Oxidized 1-Palmitoyl-2-arachidonoyl-sn-glycero-3-phosphocholine
TER	transendothelial electrical resistance
VE	cadherin - vascular endothelial cadherin
XPerT	express permeability testing assay

References

1. Beckers CM, van Hinsbergh VW, van Nieuw Amerongen GP. Thromb Haemost. 2010; 103(1):40–55. [PubMed: 20062930]
2. Spindler V, Schlegel N, Waschke J. Cardiovasc Res. 2010; 87(2):243–253. [PubMed: 20299335]
3. Murthy KS. Annu Rev Physiol. 2006; 68:345–374. [PubMed: 16460276]
4. Bass MD, Morgan MR, Roach KA, Settleman J, Goryachev AB, Humphries MJ. J Cell Biol. 2008; 181(6):1013–1026. [PubMed: 18541700]
5. Guilluy C, Swaminathan V, Garcia-Mata R, O'Brien ET, Superfine R, Burridge K. Nat Cell Biol. 2011; 13(6):722–727. [PubMed: 21572419]
6. Birukova AA, Malyukova I, Poroyko V, Birukov KG. Am J Physiol Lung Cell Mol Physiol. 2007; 293(1):L199–211. [PubMed: 17513457]
7. Birukova AA, Zebda N, Fu P, Poroyko V, Cokic I, Birukov KG. J Cell Physiol. 2011; 226(8):2052–2062. [PubMed: 21520057]
8. Birukova AA, Singleton PA, Gawlak G, Tian X, Mirzapoiazova T, Mambetsariev B, Dubrovskyi O, Oskolkova OV, Bochkov VN, Birukov KG. Mol Biol Cell. 2014; 25(13):2006–2016. [PubMed: 24829380]
9. Singleton PA, Dudek SM, Chiang ET, Garcia JG. Faseb J. 2005; 19(12):1646–1656. [PubMed: 16195373]
10. Wang L, Dudek SM. Microvasc Res. 2009; 77(1):39–45. [PubMed: 18973762]
11. Birukova AA, Alekseeva E, Mikaelyan A, Birukov KG. FASEB J. 2007; 21(11):2776–2786. [PubMed: 17428964]
12. Tian Y, Gawlak G, Shah AS, Higginbotham K, Tian X, Kawasaki Y, Akiyama T, Sacks DB, Birukova AA. J Biol Chem. 2015; 290(7):4097–4109. [PubMed: 25492863]
13. Tian X, Tian Y, Gawlak G, Meng F, Kawasaki Y, Akiyama T, Birukova AA. Mol Biol Cell. 2015; 26(4):636–650. [PubMed: 25518936]
14. Dudek SM, Jacobson JR, Chiang ET, Birukov KG, Wang P, Zhan X, Garcia JG. J Biol Chem. 2004; 279(23):24692–24700. [PubMed: 15056655]
15. Leerberg JM, Yap AS. Protoplasma. 2012; 250(4):817–829. [PubMed: 23274283]
16. Bakolitsa C, Cohen DM, Bankston LA, Bobkov AA, Cadwell GW, Jennings L, Critchley DR, Craig SW, Liddington RC. Nature. 2004; 430(6999):583–586. [PubMed: 15195105]
17. Carisey A, Ballestrem C. Eur J Cell Biol. 2011; 90(2–3):157–163. [PubMed: 20655620]
18. Goldmann WH, Auernheimer V, Thievessen I, Fabry B. Cell Biol Int. 2013; 37(5):397–405. [PubMed: 23494917]
19. Mohl C, Kirchgessner N, Schafer C, Kupper K, Born S, Diez G, Goldmann WH, Merkel R, Hoffmann B. Cell Motil Cytoskeleton. 2009; 66(6):350–364. [PubMed: 19422016]
20. Weiss EE, Kroemker M, Rudiger AH, Jockusch BM, Rudiger M. J Cell Biol. 1998; 141(3):755–764. [PubMed: 9566974]
21. Watabe-Uchida M, Uchida N, Imamura Y, Nagafuchi A, Fujimoto K, Uemura T, Vermeulen S, van Roy F, Adamson ED, Takeichi M. J Cell Biol. 1998; 142(3):847–857. [PubMed: 9700171]
22. Huveneers S, Oldenburg J, Spanjaard E, van der Krogt G, Grigoriev I, Akhmanova A, Rehmann H, de Rooij J. J Cell Biol. 2012; 196(5):641–652. [PubMed: 22391038]
23. Bochkov VN, Mechtcheriakova D, Lucerna M, Huber J, Malli R, Graier WF, Hofer E, Binder BR, Leitinger N. Blood. 2002; 99(1):199–206. [PubMed: 11756172]
24. Leitinger N, Tyner TR, Oslund L, Rizza C, Subbanagounder G, Lee H, Shih PT, Mackman N, Tigyi G, Territo MC, Berliner JA, Vora DK. Proc Natl Acad Sci U S A. 1999; 96(21):12010–12015. [PubMed: 10518567]
25. Watson AD, Leitinger N, Navab M, Faull KF, Horkko S, Witztum JL, Palinski W, Schwenke D, Salomon RG, Sha W, Subbanagounder G, Fogelman AM, Berliner JA. J Biol Chem. 1997; 272(21):13597–13607. [PubMed: 9153208]
26. Humphries JD, Wang P, Streuli C, Geiger B, Humphries MJ, Ballestrem C. J Cell Biol. 2007; 179(5):1043–1057. [PubMed: 18056416]

27. Birukova AA, Zebda N, Cokic I, Fu P, Wu T, Dubrovskyi O, Birukov KG. Exp Cell Res. 2011; 317(6):859–872. [PubMed: 21111731]
28. Singleton PA, Chatchavalvanich S, Fu P, Xing J, Birukova AA, Fortune JA, Klibanov AM, Garcia JG, Birukov KG. Circ Res. 2009; 104(8):978–986. [PubMed: 19286607]
29. Birukova AA, Birukov KG, Smurova K, Adyshev DM, Kaibuchi K, Alieva I, Garcia JG, Verin AD. FASEB J. 2004; 18(15):1879–1890. [PubMed: 15576491]
30. Birukova AA, Smurova K, Birukov KG, Usatyuk P, Liu F, Kaibuchi K, Ricks-Cord A, Natarajan V, Alieva I, Garcia JG, Verin AD. J Cell Physiol. 2004; 201(1):55–70. [PubMed: 15281089]
31. Birukov KG, Jacobson JR, Flores AA, Ye SQ, Birukova AA, Verin AD, Garcia JG. Am J Physiol Lung Cell Mol Physiol. 2003; 285(4):L785–797. [PubMed: 12639843]
32. Birukova AA, Moldobaeva N, Xing J, Birukov KG. Am J Physiol Lung Cell Mol Physiol. 2008; 295(4):L612–623. [PubMed: 18689603]
33. Bays JL, Peng X, Tolbert CE, Guilluy C, Angell AE, Pan Y, Superfine R, Burridge K, DeMali KA. J Cell Biol. 2014; 205(2):251–263. [PubMed: 24751539]
34. Birukov KG, Bochkov VN, Birukova AA, Kawkitinarong K, Rios A, Leitner A, Verin AD, Bokoch GM, Leitinger N, Garcia JG. Circ Res. 2004; 95(9):892–901. [PubMed: 15472119]
35. Birukova AA, Smurova K, Birukov KG, Kaibuchi K, Garcia JGN, Verin AD. Microvasc Res. 2004; 67(1):64–77. [PubMed: 14709404]
36. Totsukawa G, Yamakita Y, Yamashiro S, Hartshorne DJ, Sasaki Y, Matsumura F. J Cell Biol. 2000; 150(4):797–806. [PubMed: 10953004]
37. Sanders LC, Matsumura F, Bokoch GM, de Lanerolle P. Science. 1999; 283(5410):2083–2085. [PubMed: 10092231]
38. Arce FT, Whitlock JL, Birukova AA, Birukov KG, Arnsdorf MF, Lal R, Garcia JG, Dudek SM. Biophys J. 2008; 95(2):886–894. [PubMed: 18408039]
39. Birukova AA, Arce FT, Moldobaeva N, Dudek SM, Garcia JG, Lal R, Birukov KG. Nanomedicine. 2009; 5(1):30–41. [PubMed: 18824415]
40. Krishnan R, Klumpers DD, Park CY, Rajendran K, Trepat X, van Bezu J, van Hinsbergh VW, Carman CV, Brain JD, Fredberg JJ, Butler JP, van Nieuw Amerongen GP. Am J Physiol Cell Physiol. 2011; 300(1):C146–154. [PubMed: 20861463]
41. Pesen D, Hoh JH. Biophys J. 2005; 88(1):670–679. [PubMed: 15489304]
42. Xu M, Waters CL, Hu C, Wysolmerski RB, Vincent PA, Minnear FL. Am J Physiol Cell Physiol. 2007; 293(4):C1309–1318. [PubMed: 17670896]
43. Ando K, Fukuhara S, Moriya T, Obara Y, Nakahata N, Mochizuki N. J Cell Biol. 2013; 202(6): 901–916. [PubMed: 24019534]
44. Carisey A, Tsang R, Greiner AM, Nijenhuis N, Heath N, Nazgiewicz A, Kemkemer R, Derby B, Spatz J, Ballestrem C. Curr Biol. 2013; 23(4):271–281. [PubMed: 23375895]
45. Barry AK, Wang N, Leckband DE. J Cell Sci. 2015; 128(7):1341–1351. [PubMed: 25663699]
46. del Rio A, Perez-Jimenez R, Liu R, Roca-Cusachs P, Fernandez JM, Sheetz MP. Science. 2009; 323(5914):638–641. [PubMed: 19179532]
47. Dubrovskyi O, Tian X, Poroyko V, Yakubov B, Birukova AA, Birukov KG. FEBS Lett. 2012; 586(16):2294–2299. [PubMed: 22728435]
48. Peng X, Cuff LE, Lawton CD, DeMali KA. J Cell Sci. 2010; 123(Pt 4):567–577. [PubMed: 20086044]
49. Sun X, Shikata Y, Wang L, Ohmori K, Watanabe N, Wada J, Shikata K, Birukov KG, Makino H, Jacobson JR, Dudek SM, Garcia JG. Microvasc Res. 2009; 77(3):304–313. [PubMed: 19323978]
50. Zhang H, Webb DJ, Asmussen H, Niu S, Horwitz AF. J Neurosci. 2005; 25(13):3379–3388. [PubMed: 15800193]
51. le Duc Q, Shi Q, Blonk I, Sonnenberg A, Wang N, Leckband D, de Rooij J. J Cell Biol. 2010; 189(7):1107–1115. [PubMed: 20584916]
52. Tornavaca O, Chia M, Dufton N, Almagro LO, Conway DE, Randi AM, Schwartz MA, Matter K, Balda MS. J Cell Biol. 2015; 208(6):821–838. [PubMed: 25753039]

Highlights

- Barrier-protective (OxPAPC) and and barrier-disruptive (thrombin) agonists induced different patterns of focal adhesion remodeling.
- Knockdown of vinculin attenuated both, OxPAPC-induced decrease and thrombin-induced increase in endothelial permeability.
- In both scenarios, vinculin association with focal adhesions and adherens junctions controls cytoskeletal tension which is required for both, barrier enhancing and barrier disruptive endothelial response.

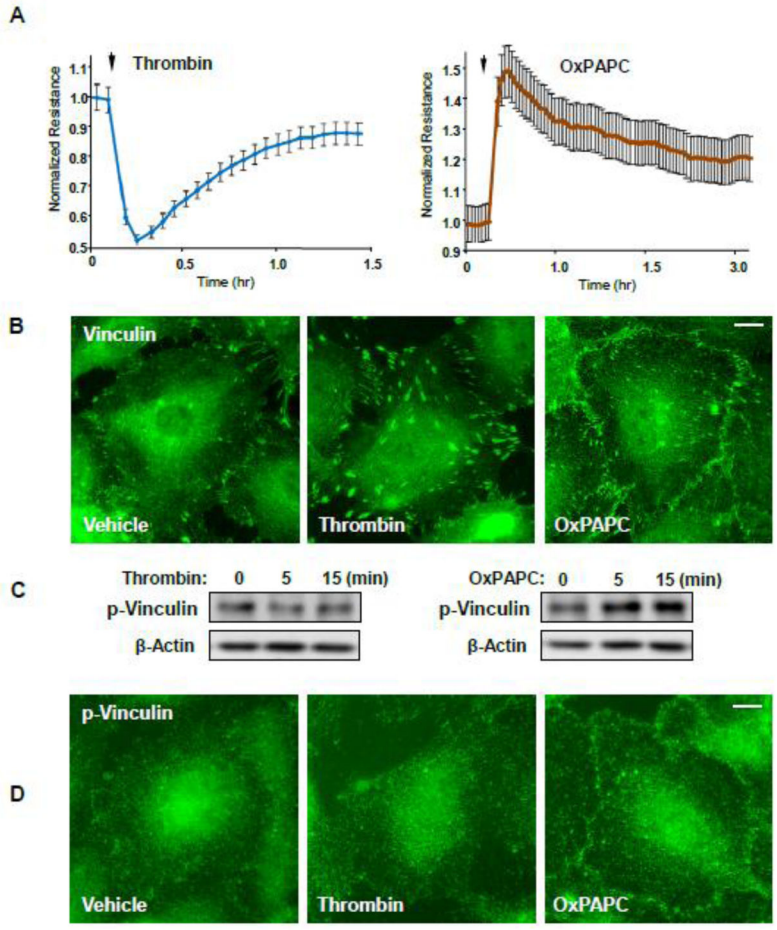

Figure 1. Effects of thrombin and OxPAPC on endothelial permeability and vinculin distribution

A - HPAEC plated on microelectrodes were treated with thrombin (0.2 U/ml) or OxPAPC (15 μg/ml) followed by TER measurements. The TER curves represent pooled data from three independent experiments. **B** - Cells grown on glass coverslips were stimulated with thrombin or OxPAPC for 15 or 30 min, respectively. Vinculin localization was analyzed by immunofluorescence staining with corresponding antibody. Results are representative of three independent experiments. **C** - Western blot analysis of phospho-Y822 vinculin levels in HPAEC stimulated with thrombin (0.2 U/ml) or OxPAPC (15 μg/ml) at the indicated time points. **D** - Cells grown on glass coverslips were stimulated with thrombin or OxPAPC for 5 or 15 min, respectively. Phospho-Y822 vinculin localization was analyzed by immunofluorescence staining with corresponding antibody. Bar - 5 μm. Results are representative of three independent experiments.

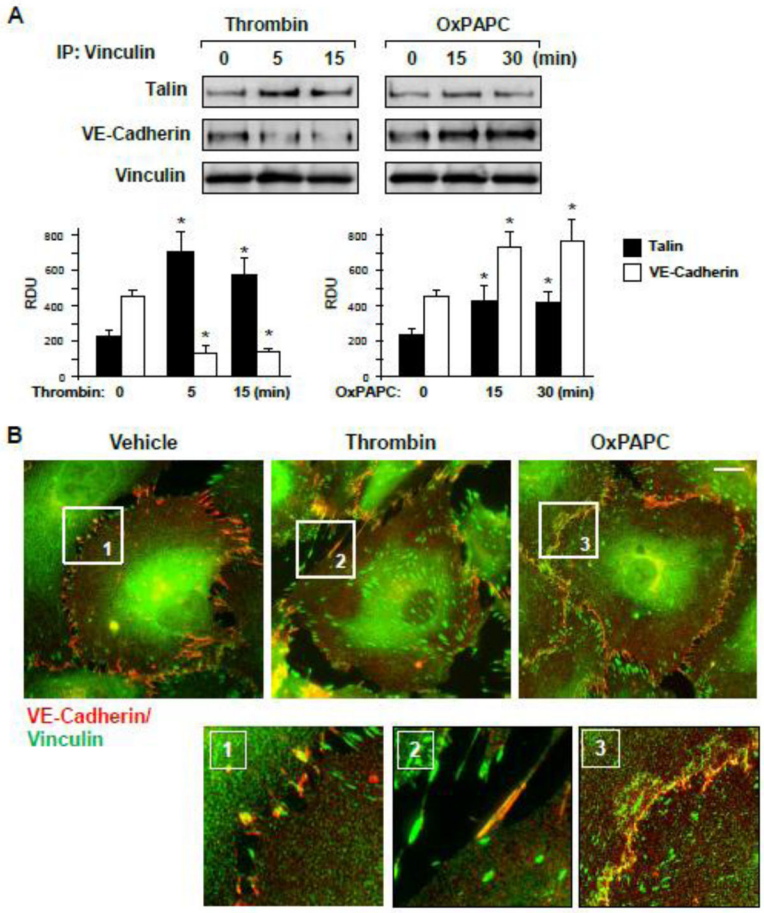

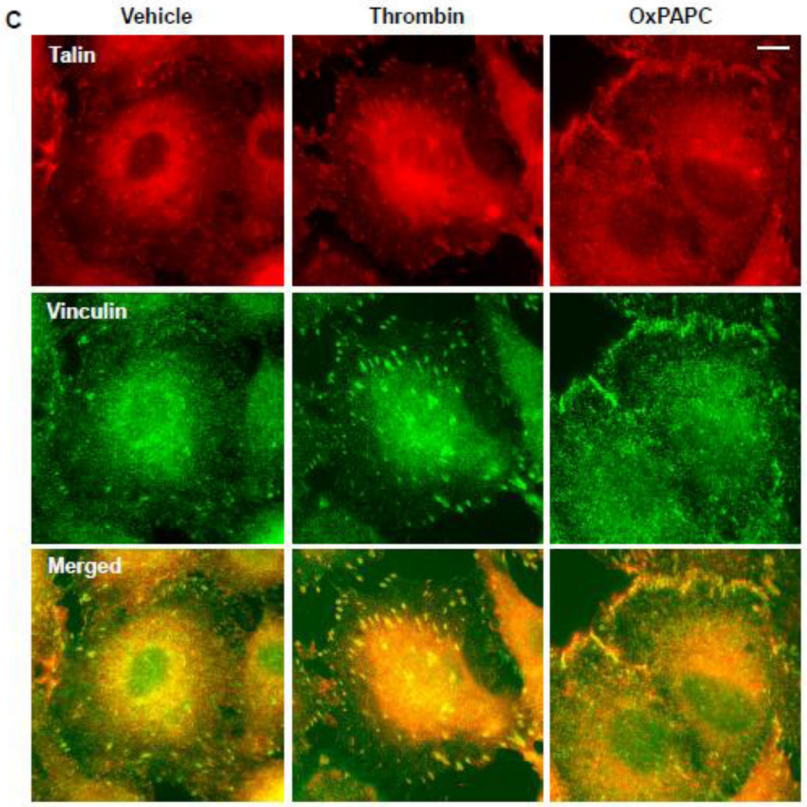

Figure 2. Effects of thrombin and OxPAPC on focal adhesion and adherens junction remodeling

A – EC were stimulated with thrombin (0.2 U/ml) or OxPAPC (15 μg/ml), followed by vinculin immunoprecipitation under non-denaturing conditions. Presence of talin and VE-cadherin in immune complexes was tested by Western blot. Bar graphs depict quantitative analysis of Western blot data; n=3; *P<0.05 vs. vehicle. **B and C –** Thrombin- or OxPAPC-induced vinculin redistribution and its colocalization with VE-cadherin (**B**) and talin (**C**) was evaluated by immunofluorescence staining of formaldehyde-fixed EC for vinculin (green) and VE-cadherin or talin (red). Bar - 5 μm. Higher magnification insets show details of vinculin and VE-cadherin co-localization (yellow). Results are representative of three to five independent experiments.

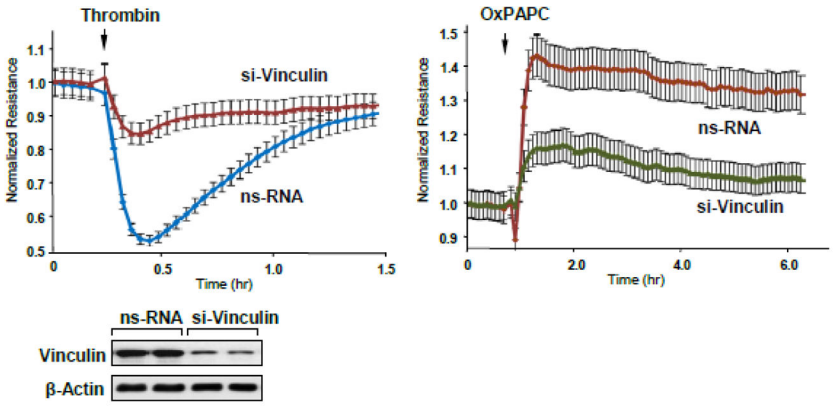

Figure 3. Effects of vinculin knockdown on thrombin and OxPAPC permeability response

Human pulmonary EC were transfected with vinculin-specific or non-specific siRNA. TER was measured in EC stimulated with thrombin (0.2 U/ml) or OxPAPC (15 μg/ml). The TER curves represent pooled data from three independent experiments. siRNA-induced vinculin protein depletion was confirmed by western blot.

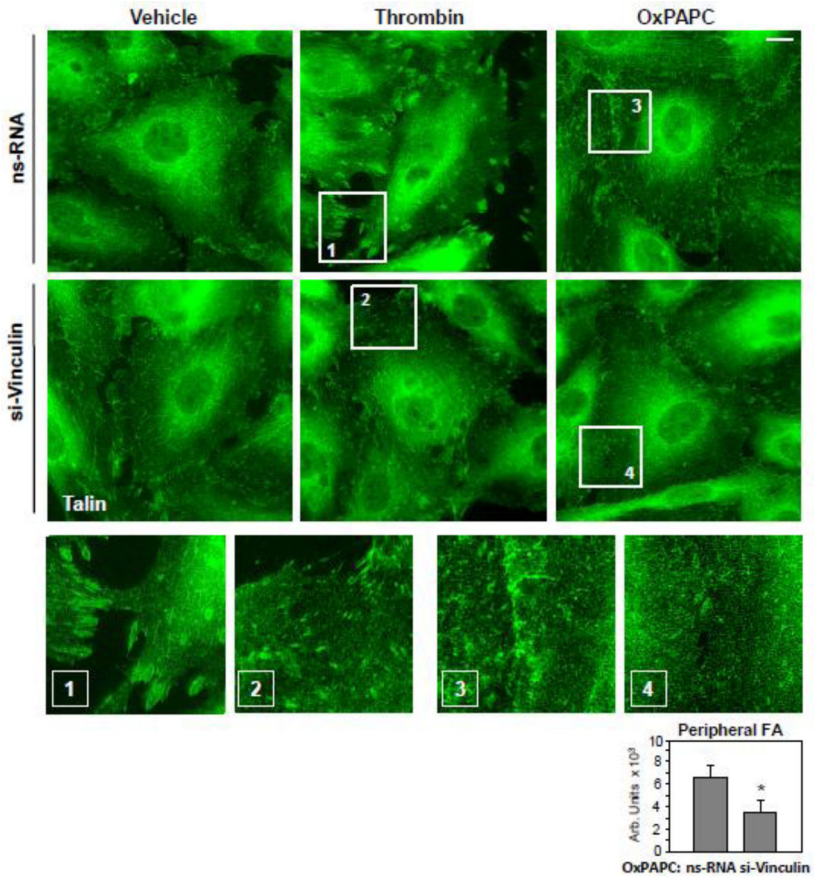

Figure 4. Effect of vinculin knockdown on agonist-induced focal adhesion remodeling

Human pulmonary EC were transfected with vinculin-specific or non-specific siRNA. Focal adhesion remodeling in response to thrombin treatment (0.2 U/ml, 10 min) or OxPAPC (15 μg/ml, 30 min) treatment was analyzed by immunofluorescence staining for talin. Bar - 5 μm. Higher magnification insets show details of focal adhesion remodeling in control and stimulated EC. Bar graph represents quantitative analysis of OxPAPC-induced peripheral accumulation of focal adhesions in control and vinculin-depleted EC. Results are representative of four independent experiments.

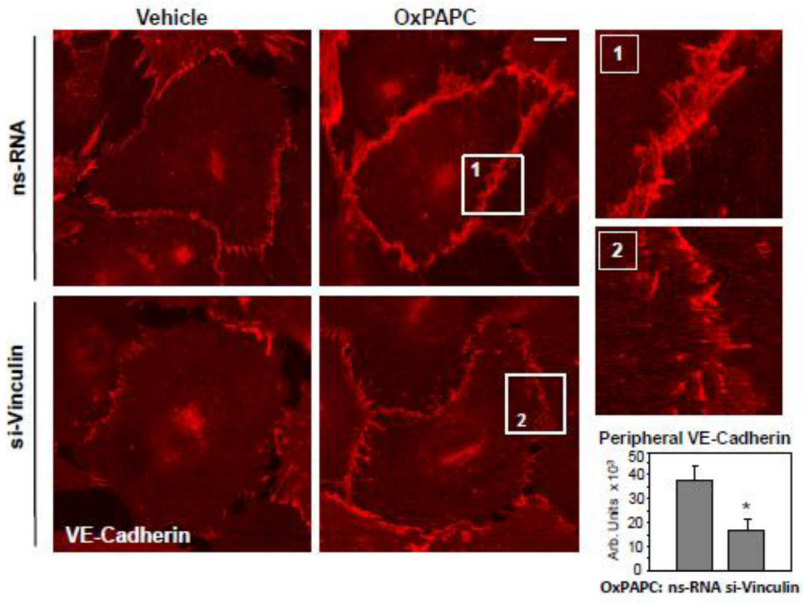

Figure 5. Effect of vinculin knockdown on OxPAPC-induced adherens junction remodeling

Human pulmonary EC were transfected with vinculin-specific or non-specific siRNA. Adherens junction remodeling in response to OxPAPC (15 μg/ml, 30 min) was analyzed by immunofluorescence staining for VE-cadherin. Bar - 5 μm. Higher magnification insets show details of adherens junction remodeling in control and stimulated EC. Bar graph represents quantitative analysis of the areas covered by adherens junctions in control and vinculin-depleted EC stimulated with OxPAPC. Results are representative of four independent experiments.

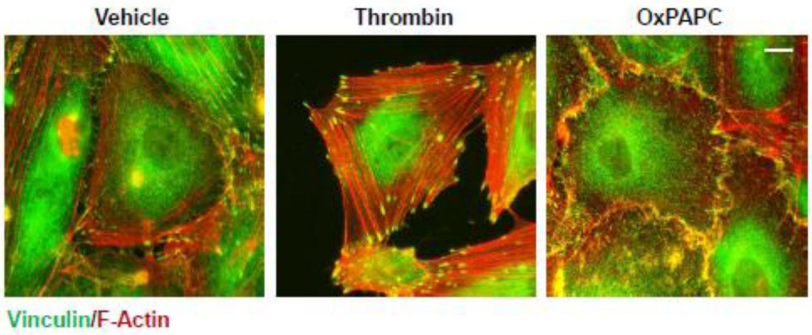

Figure 6. Analysis of cytoskeletal remodeling in response thrombin and OxPAPC

HPAEC grown on glass coverslips were stimulated thrombin treatment (0.2 U/ml, 10 min) or OxPAPC (15 μg/ml, 30 min) followed by double immunofluorescence staining for F-actin (red) and vinculin (green). Areas of actin and vinculin co-localization appear in yellow. Bar - 5 μm. Results are representative of three independent experiments.

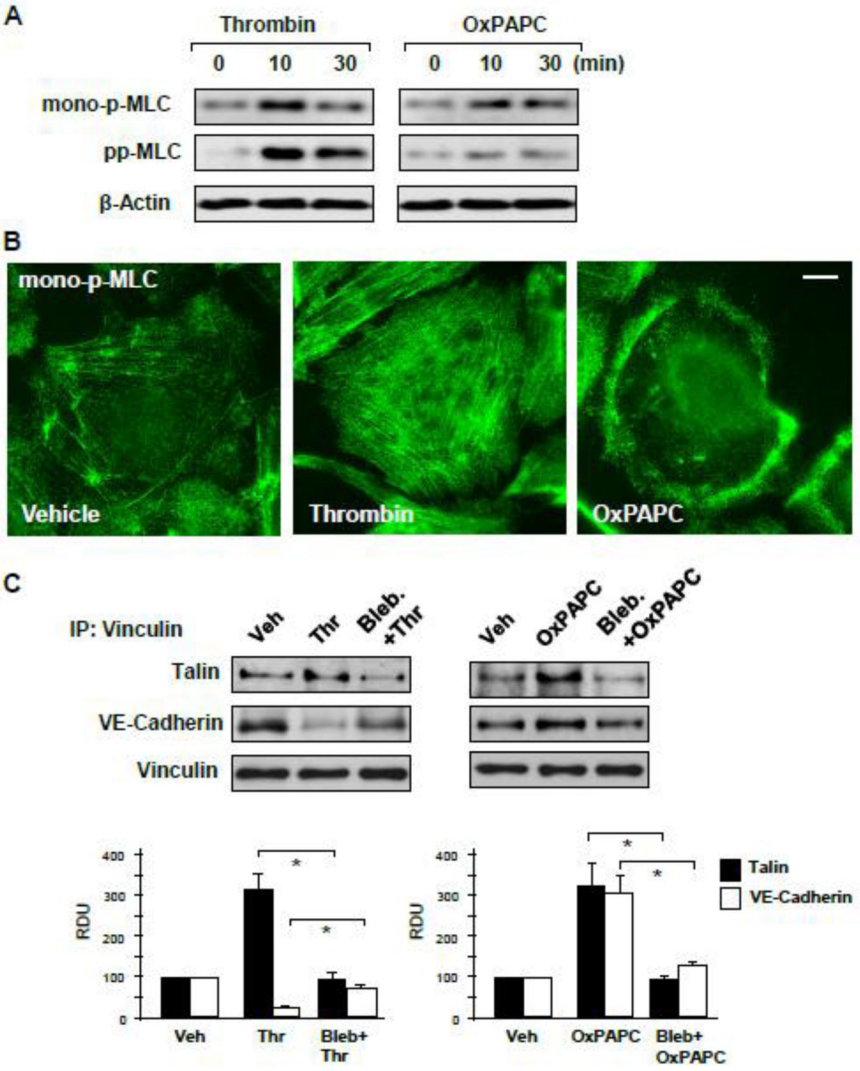

Figure 7. Analysis of contractile signaling in response to thrombin and OxPAPC

A – MLC mono- and di-phosphorylation was analyzed by Western blotting with corresponding antibodies in control, thrombin (0.2 U/ml) or OxPAPC (15 μg/ml) treated EC. Probing for β-actin was used as a normalization control. **B –** Intracellular localization of mono-phosphorylated MLC in control and agonist-stimulated cells (thrombin 10 min, OxPAPC 30 min) was determined by immunofluorescence staining with specific antibody. Bar - 5 μm. **C –** HPAEC were pretreated with vehicle or blebbistatin (15 μM, 30 min), followed by stimulation with thrombin (0.2 U/ml, 10 min) or OxPAPC (15 μg/ml, 30 min). Co-immunoprecipitation assays using vinculin antibody were performed, and talin and VE-cadherin content in the immunoprecipitates was detected using appropriate antibody. Bar graphs depict quantitative analysis of Western blot data; n=3; *P<0.05 vs. thrombin or OxPAPC alone.

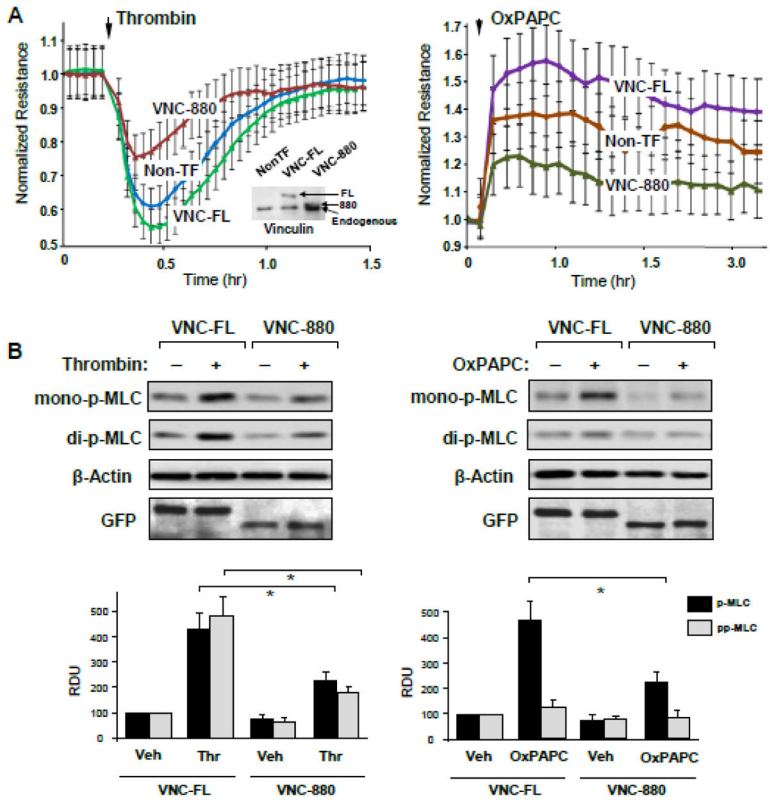

Figure 8. Effect of vinc880 mutant on thrombin- and OxPAPC-induced alterations of EC permeability

HPAEC were transfected with full length (VNC-FL) or vinculin-880 (VNC-880) mutant or left un-transfected followed by stimulation with thrombin (0.2 U/ml) or OxPAPC (15 μg/ml). **A –** TER measurements were performed over the time indicated. The TER curves represent pooled data from three independent experiments. Inset: The levels of ectopically expressed GFP-tagged wild type and vinculin-880 mutant as well as endogenous vinculin were detected by immunoblotting using anti-GFP and vinculin antibodies. **B** - Cells were stimulated with thrombin or OxPAPC for 10 min or 30 min, respectively. Western blot analysis of agonist-induced mono- and di-phosphorylation of MLC. Probing for β-actin was used as a normalization control. Bar graphs depict quantitative analysis of Western blot data; n=3; *P<0.05 vs. VNC-FL.